CHEMISTRY
A EUROPEAN JOURNAL

FULL PAPER

DOI: 10.1002/chem.200((will be filled in by the editorial staff))

Modified SWCNTs with Amphoteric Redox and Solubilizing Properties

Laura Rodríguez-Pérez,[a] Raúl García,[a] Mª Ángeles Herranz*[a] and Nazario Martín*[a, b]

A complementary double covalent functionalization of SWCNTs involving both solubilizing ionic liquids and electroactive moieties is reported. Our strategy is a simple and efficient methodology based on the stepwise functionalization of the nanotube surface with two different organic moieties. In a first instance, oxidized SWCNTs are amidated with ionic liquid moieties, and further reacted with *n*-butyl bromide affording 1-butylimidazolium bromide salt-functionalized SWCNTs. This allows a tuneable polarity induced by anion exchange, having an effect on the relative solubility of the modified SWCNTs on water. Subsequently, a 1,3-dipolar cycloaddition reaction was performed to introduce the electron acceptor tetracyanoanthra-*p*-quinodimethane (TCAQ) unit on the SWCNTs. Furthermore, to evaluate the influence of the functional groups position, the TCAQ electroactive molecule has been anchored through esterification reaction onto previously oxidized SWCNTs, followed by Tour reaction to introduce the ionic liquid functions. Infrared and Raman spectroscopies, thermogravimetric analysis (TGA), Steady-state UV-vis-NIR spectroscopy, transmission electron microscopy (TEM), and X-ray photoelectron spectroscopy (XPS) clearly confirmed the double covalent functionalization of SWCNTs.

Keywords: double functionalization • single wall carbon nanotubes • ionic liquids • electron-acceptors • solubility switching

Introduction

Since their discovery by S. Iijima in 1991,[1] carbon nanotubes (CNTs) are among the materials of choice for applications in nanotechnology due to the chemical stability, excellent mechanical properties, high surface area and thermal conductivity that they exhibit.[2,3] In particular, 1-D single-wall carbon nanotubes (SWCNTs) display a variety of novel properties which make them very appealing carbon nanoforms.[4] However, one major drawback of SWCNTs is their difficult processability and/or dispersibility stemming from the inert and apolar character of their surface. In this frame, SWCNTs chemical functionalization with covalent methods has significantly enhanced the solubility in various solvents and produced novel, robust and more sophisticated hybrid materials, free of aggregates and bundles, potentially suitable for further applications.[5]

On the other hand, Ionic Liquids (ILs) have gained a wide popularity within the scientific community due to their importance in a broad range of applications.[6] This molten salts based on organic cations and inorganic or organic anions, constitute an innovative and environmental friendly reaction medium due to their unique and singular properties such as low melting points, typically below room temperature, and high thermal stability.[7] Their physicochemical properties, specifically the ILs polarity, can easily be turned by designing their structure, namely choosing the right combination of cations and anions. In this regard, imidazolium salts composed of imidazolium-based cations have been combined with CNTs providing them with different hydrophobicity/hydrophilicity character,[8,9] charge transfer activity[8] or gel behavior.[10] Moreover, this powerful strategy may improve the dispersion and solubilization of SWCNTs,[11] at the time that allows the combination of the SWCNTs and IL properties to those of other materials facilitating the development of functional structures.

Several approaches have been investigated for the double or triple functionalization of CNTs and the introduction of multipurpose, versatile synthons.[12] In particular, this strategy has resulted particularly beneficial for biological applications,[13] where the possibility of covalently attach a drug, a targeting ligand and a fluorophore has recently been accomplished.[14] However, mixed covalent methodologies have not been investigated so far in the search for practical architectures where photo and/or redox active building blocks are connected to SWCNTs and their stability, solubility and electronic interactions adjusted by a secondary functionalization.

[a] Dr. L. Rodríguez-Pérez. Dr. Raúl García, Dr. Mª Ángeles Herranz, Prof. Dr. N. Martin. Departamento de Química Orgánica I, Facultad de Ciencias Quimicas
Universidad Complutense de Madrid, 28040 Madrid (Spain)
Fax: (+34) 91-394-4103, E-mail: maherran@quim.ucm.es, nazmar@quim.ucm.es,
Homepage: http://www.ucm.es/info/fullerene/

[b] Prof. Dr. N. Martin.
IMDEA-Nanoscience
C/Faraday, 9. Ciudad Universitaria de Cantoblanco, 28049 Madrid (Spain)

Supporting information for this article is available on the WWW under http://www.chemeurj.org/ or from the author.

Although various *n*-type electron-acceptors have been bound to SWCNTs by using non-covalent interactions,[15] the covalent approach has been scarcely investigated towards the electron donating ability of SWCNTs.[4] We have recently explored the *p*-doping of SWCNTs with the *n*-type electron-acceptor unit 11,11,12,12-tetracyano-9,10-anthra-*p*-quinodimethane (TCAQ) considering a supramolecular approach and, demonstrated that this electroactive unit effectively individualizes SWCNTs when combined with a dendronized core.[16] The TCAQ family provides suitable electron-acceptor systems that have been investigated as strong electron acceptors in charge-transfer complexes or at metal interfaces, as well as, covalently connected to conjugated polymers and fullerenes.[17] TCAQs exhibit low reduction potential values and their central *p*-quinoid moiety confers high stability to the aromatic reduced species.[18]

In the present work, we focused our attention on the synthesis, characterization and properties of covalently double functionalized SWCNTs conjugates bearing 1-butyl-3-methylimidazolium hexafluorophosphate (BMIM PF_6) ionic liquid analogues and TCAQ units. The ionic liquid moieties covalently linked to the surface may allow a reversibly switchable solubility between aqueous and organic solvents induced by anion exchange, while the TCAQs introduce a specific electroactivity to the system acting as *n*-type dopants, forcing the SWCNTs to acts as electron donor species.

Results and Discussion

The synthetic pathway toward SWCNTs conjugates **4a,b** is summarized in Scheme 1. Prior to use, the raw material containing approximately ~90% of SWCNTs was purified by an optimized soft acidic treatment. Briefly, pristine SWCNTs (HiPCO) were dispersed in HNO_3 and heated at reflux for 24 h, followed by filtration and extensive washing with water until neutral pH. Under these conditions, the SWCNTs undergo an oxidation process, introducing covalent functionalities, mainly carboxylic acid groups, which activate their surface.[19] The oxidized SWCNTs **1** were further functionalized with imidazole moieties through an amidation reaction.[20] To attain the amide formation, the first step consists in the conversion of the carboxylic acid groups to acid chlorides using an excess of thionyl chloride. These suitably functionalized carbon nanotubes react with an excess of 3-(aminopropyl)imidazole at 120 °C for 24 h under inert atmosphere. The resulting product (**2**) was purified by washing with plenty of THF. Afterwards, the double functionalization was introduced using 1,3-dipolar cycloaddition reactions[21] with *N*-methylglycine (sarcosine) and 4-cyanobenzaldehyde (**3a**) or 2-formyl-11,11,12,12-tetracyano-9,10-anthra-*p*-quinodimethane (**3b**), respectively, through the in situ formation of the corresponding azomethine ylides. The ionic functionalized SWCNTs **4a,b** were obtained treating **3a,b** with an excess of *n*-butyl bromide, followed by anion exchange reaction with potassium hexafluorophosphate.[22]

The preparation of **3a** and **4a** was used as a control methodology, since 4-cyanobenzaldehyde is commercially available and bears a cyano group, such as those of TCAQ, that can be identified by different spectroscopic and analytical techniques (Figures S1 - S5). Once established the protocol, to synthesize the functionalized SWCNTs **3b** endowed with TCAQ units, the 1,3-dipolar cycloaddition reaction of *N*-methylglycine and the formyl-containing TCAQ with **2** was carried out in *o*-dichlorobenzene (*o*-DCB) under horn ultrasonication. Once the reaction was completed, most of the physically adsorbed organic materials were removed by filtration and washed with organic solvents (*o*-DCB, DCM, acetone, methanol). In order to obtain the charged species, the resulting material (**3b**) was treated with an excess of *n*-butyl bromide. Finally, as mentioned above, an exchange reaction with potassium hexafluorophosphate led to **4b**. In a separate experiment, the TCAQ organic molecule behaviour during the ultrasonication process in *o*-DCB was also studied, revealing the stability of this compound after 48 h of reaction by TLC.

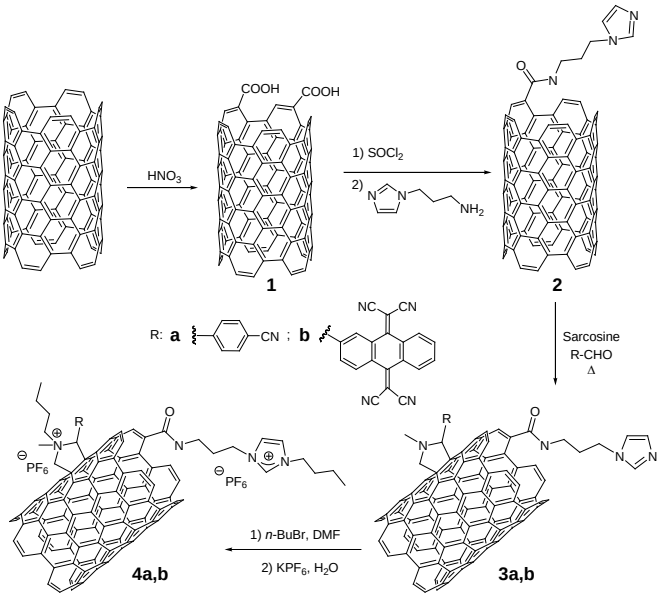

Scheme 1. Chemical structures and reaction conditions for the preparation of double functionalized SWCNTs nanoconjugates **4a,b**.

All the nanohybrid SWCNTs obtained were characterized via FTIR and Raman spectroscopies, thermogravimetric analysis (TGA), UV-vis-NIR absorption spectroscopy , X-ray photoelectron spectroscopy (XPS), and transmission electron microscopy (TEM) to obtain fully detailed information about the structural, electronic and chemical properties of the functionalized carbon nanotubes.

The FTIR spectra give evidence of the functional groups that were introduced on the SWCNTs skeleton (Figure 1). In particular, the band due to the skeletal in-plane vibration at 1592 $cm^{-1}$of the pristine SWCNTs is easily recognized, SWCNTs-COOH **1** show features that do not appear on pristine SWCNTs such as two bands at 1723 cm^{-1} (C=O) and at 1200 cm^{-1} (C–O stretching) attributed to the carboxylic groups. For **2**, the effective grafting of the imidazolium functionalities onto the CNT surface is confirmed by the presence of the amide band at 1668 cm^{-1}, the aliphatic C–H stretching bands between 2850 and 2950 cm^{-1} and bands at 1250–1500 cm^{-1} assigned to C–H bending. The band at 1723 cm^{-1} of carboxylic acid group is still observed in **4b**, indicating the presence of remaining COOH groups. More interestingly, the cyano band at 2226 cm^{-1} and the P-F stretching band of the PF_6^- anion at 840 cm^{-1} are easily recognized in the FTIR spectrum of **4b** and, indicate the presence of TCAQ units and the quaternization carried out in the amines.

Raman spectroscopy complements the data obtained from FTIR and provided valuable structural information concerning the SWCNTs C-C bonds. The radial breathing modes (RBMs) bands between 186 and 270 cm^{-1} are related to SWCNTs diameter and chirality, indicating the presence of both metallic and semiconducting SWCNTs in our batch, as well as a range of diameters between 0.8 and 1.5 nm. A detailed consideration of the

RBMs (see Insert in Figure 2) reveals an increase in the RBM resonance signals of the large diameter SWCNTs (200-250 cm^{-1}) for all functionalized samples, while the resonance intensity for small diameter SWCNTs (250-300 cm^{-1}) are decreased. This effect on the RBM spectral features indicate a size selective reaction of the small diameter SWCNTs, as previously observed for other oxidation and addition reactions of SWCNTs.[23]

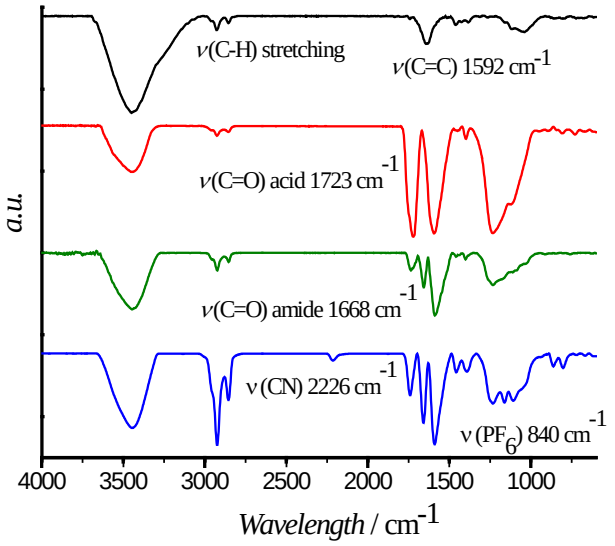

Figure 1. FTIR spectra of **4b** (blue) compared to **2** (green), **1** (red) and pristine SWCNTs

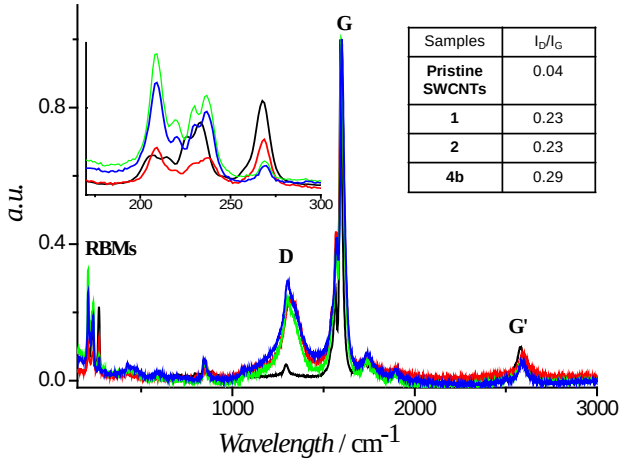

Samples	I_D/I_G
Pristine SWCNTs	0.04
1	0.23
2	0.23
4b	0.29

Figure 2. Raman spectra of pristine SWCNTs (black), **1** (red), **2** (green) and **4b** (blue). The excitation wavelength in the spectra measurement was 785 nm.

Moreover, two characteristic bands of carbon nanotubes are observed in the Raman spectra, the D mode (sp^3 carbons), defect band, located at frequencies between 1330 and 1360 cm^{-1}, due to disorder on the carbon hexagonal lattice on the CNT sidewalls, and the G mode or MT-tangential mode, corresponding to the stretching mode in the graphite (sp^2 carbons), located at 1580 cm^{-1}. The ratio of the intensities between these two bands (I_D/I_G) offers valuable information about the degree of functionalization. The increase in the I_D/I_G ratio reported in Figure 2 when passing from pristine SWNTs to **1** is caused by the change in hybridization of the carbon atoms (from sp^2 to sp^3) due to the oxidation of pristine SWCNTs (red line) and, afterwards due to the 1,3-dipolar cycloaddition reaction to yield nanohybrids **4b** (blue line), which incorporate additional pyrrolidine units on the sidewalls of the carbon nanotubes. The I_D/I_G ratio is similar for **1** and **2**, since the amidation reaction occurs on the carboxylic acid residues previously introduced.

The modification of the sp^2 skeleton of the SWCNTs is also evident in the steady state absorption spectra in the UV-vis-NIR regions because of the almost complete loss of the van Hove singularities typical of pristine SWCNTs, particularly for the double functionalized nanoconjugates **4b**.[24] (Figure S6).

Thermogravimetric analysis is an important tool for determining the purity of the SWCNTs after the nitric acid treatment. TGA analyses under oxidizing conditions (oxygen) show an improvement of purity up to 96.7 %, with only a remaining 3.3 % of iron nanoparticles, compared to pristine SWCNTs which have a purity of 92,6 % (Figure S7). Furthermore, to evaluate the thermal behaviour and relative amount of organic functionalities covalently attached on the SWCNTs surface, the samples were subjected to thermogravimetric analysis under inert atmosphere. Under these analysis conditions, it is assumed that all the organic fragments are removed without affecting the SWCNTs skeleton. A typical thermogram reveals a weight loss of 39.11 % for **4b** (Figure 3). Accordingly, it can be estimated a degree of functionalization of one unit of organic fragments per 99 carbon atoms. The functional group coverage obtained by TGA and the I_D/I_G ratio deduced from Raman spectroscopy, show a consistent trend for all the SWCNT functionalized nanohybrids (Figures 2 and 3).

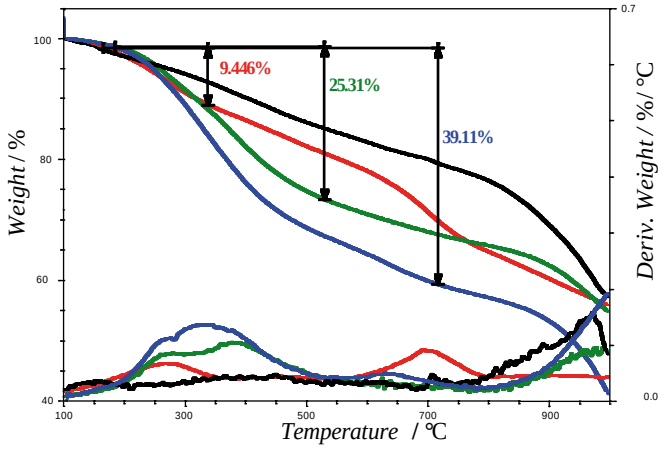

Figure 3. TGA analyses under inert atmosphere of pristine SWCNTs (black), oxidized SWCNTs (**1**) (red), **2** (green) and **4b** (blue).

XPS analysis was also employed to investigate the composition of the functionalized SWCNTs. This technique allowed us to identify the surface groups, the chemical state of the atoms, and their relative abundance in the SWCNTs nanohybrids obtained. Figure 4a shows a typical survey spectrum for **4b**, revealing peaks from C 1s (284.2 eV), N 1s (399.6 eV), O 1s (532.6 eV), and F 1s (689.6 eV), To obtain semiquantitative assessment of the degree of functionalization the XPS spectrum was normalized to the C 1s peak and ratios of a 5.3 % for N, 3.9 % for F and 23.3 % for O atoms were obtained. No signal for P 2p was obtained in the XPS analysis, due probably to the low abundance of this atom in our samples (1 P atom per 6 F). Nevertheless, the presence of N and F atoms in the

sample demonstrate that the SWCNTs have been derivatized as expected.

The high-resolution C 1s core level spectrum for sample **4b** (Figure 4b) is composed of five different components according to the peak assignment used in previous reports,[25], namely i) a main peak centred at 283.8 eV originated by the photoelectrons emitted from sp^2 carbon atoms of the graphene sheets with their π-π* shape up structure (at around 291.4 eV) indicative of the presence of carbon nanostructures; ii) a peak centred at 284.5 eV assigned to the sp^3 carbon atoms, namely from alkyl groups; iii) a component localized at 285.0 eV attributed to oxidized carbon atoms C-O bonds; iv) and v) two peaks centred at 285.6 and 287.3 eV, most probably generated by photoelectrons emitted from carbon atoms belonging to carbonyl and carboxyl groups, respectively. Interestingly, compound **2** showed similar C 1s line shape, whereas the C 1s peak of a pristine SWCNTs sample was satisfactorily fitted using only four components (i, iii, iv and v) indicating the absence of sp^3 C-atoms (Figure S8). Unfortunately, differentiating between C-N and C-O is extremely difficult in the XPS high resolution spectrum recorded for the carbon atom and, therefore, the C-N and C≡N components could not be clearly identified.[20]

For simplicity, the O 1s spectra of **4b** has been curve-resolved with only two components, the first one placed at *ca.* 531.4 eV assigned to C=O (31,2 %) surface groups, whereas the second one at *ca.* 533.1 eV is associated to C–O (62.7 %) groups (not shown).[26]

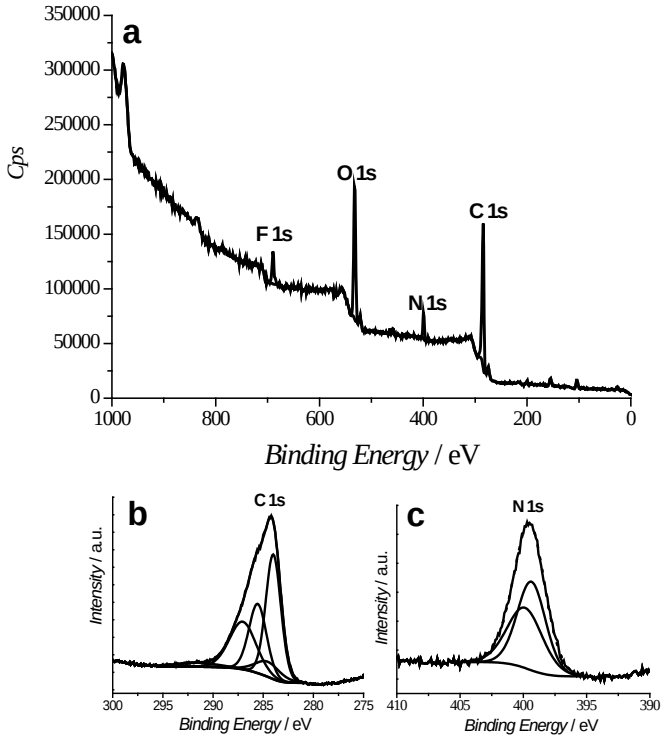

Figure 4. a) XPS survey spectrum of **4b**, b) XPS C 1s component deconvolution and, c) N 1s component deconvolution.

The N 1s peak placed at 399.7 eV could be decomposed in two different contributions for the final aggregate **4b**. The first contribution is centred at 399.3 eV (65.5 %) and could be assigned to the cyano groups of the TCAQ aggregate, the second deconvoluted peak (broader) is observed at 400.1 eV (35.6 %), and could be attributed to the amide functions and the C-N positively charged from the imidazole and the pyrrolidine functionalities.[20] Notably, the cyano nitrogens of the TCAQ units in nanoconjugate **4b** increase their binding energy by ~ 0.6–1.3 eV when compared with the reference electron-acceptor molecules. This shift is attributed to charge transfer from the SWCNTs to the TCAQ units, as recently documented for related systems.[17b,27]

The morphology of the ionic functionalized SWCNTs **4b** has also been investigated using transmission electron microscopy (TEM). Small SWCNTs bundles of 10 to 4 nm as well as debundled ones can be observed on the functionalized sample (Figure S9, right), in contrast to pristine SWCNTs where large bundles are common (Figure S9, left). This observation is consistent with the double SWCNTs functionalization, where the differently connected units may disrupt the strong interactions between individual SWCNTs.

Finally, the modification of the ionic liquid counter anion greatly changes the SWCNTs dispersability in different solvents.[28] Figure 5 shows images of solutions of functionalized SWCNTs: (a) oxidized (**1**), (b) **4b** with X = Br^- and (c) **4b** with X = PF_6^- dispersed in a two-phase mixture of H_2O and DCM. SWCNTs **1** form a homogeneous black aqueous solution in water, although its dispersion is quite instable. Modification by ILs with Br^- as counter anion retains its water solubility. In contrast, SWCNTs substituted with the lipophilic anion PF_6^- are not water soluble although can be easily dispersed in DCM. Thus, as expected, the solubility/dispersability can be altered by anion exchange. Changes in the organic molecule nature of the SWCNTs sidewall functionalization do not alter the modular behaviour inferred by the ionic liquid moiety as shown by the photographs presented in Figure 5. Similar results were obtained for the control SWCNTs functionalized material **4a**.

Figure 5. Photographs of SWCNTs nanoconjugates dispersed in H_2O (upper phase) and CH_2Cl_2 (lower phase). a) SWCNTs-COOH (**1**), b) **4b**, and d) **4a** with X=Br^-. c) **4b** and e) **4a** with X=PF_6^-.

With the aim of studying the influence of the ionic liquid position on the SWCNTs aggregates dispersibility, we have performed an interchange between both functionalities: ionic liquids and TCAQ. In this approach, the ionic liquid moiety is linked via a modified Tour reaction and, in turn, the electroactive TCAQ unit through an esterification reaction of the previously oxidized carbon nanotubes (Scheme 2). For that purpose, oxydized SWCNTs (**1**), synthesized as previously described, were functionalized by adding 1,3-aminopropyl imidazole and isoamyl nitrite in water under inert atmosphere.[29] A water suspension of **1** was sonicated in an ultrasonic processor for 30 minutes in order to obtain a homogeneous dispersion. The solution was deoxygenated prior to add the 1,3-aminopropyl imidazole and the isoamyl nitrite and, afterwards, heated at 70 ºC overnight. The functionalized SWCNTs obtained (**5**) were further reacted with 2-hydroxymethyl-TCAQ by an esterification reaction. The reaction was performed using thionyl chloride to activate the carboxylic acid groups, followed by the

esterification in THF at 70 ºC under argon atmosphere to yield the aggregates **6**. The resulting product was quaternized with *n*-BuBr and the counter anion changed with KPF_6 to provide the ionic double functionalized SWCNTs **7**.[22]

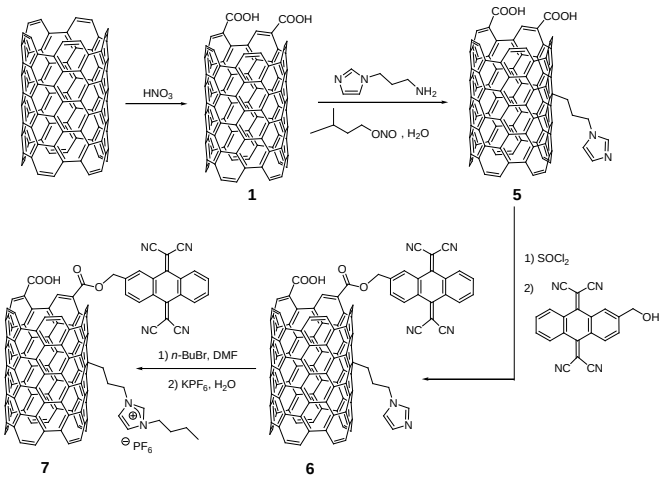

Scheme 2. Chemical structures and reaction conditions for the preparation of double functionalized SWCNTs nanoconjugates **7**.

The functionalization of the different aggregates was evidenced considering the analysis techniques mentioned above. The samples were characterized by FTIR spectroscopy where it is noticeably the appearing of the cyano band at 2226 cm^{-1} and the stretching band of the P-F at 840 cm^{-1} for **7** (Figure S10). In addition, the Raman spectra exhibit an increase in the D band from the oxidized SWCNTs to the double functionalized systems, highlighting the covalent character of the different bonds (Figure S11). The TGA analysis is also in agreement with the Raman results, evidencing a weight loss of a 34.20 % for **7** compared with the 39.11 % obtained for **4b** (Figure S12).

To evaluate the presence of structural and morphological changes of SWCNTs after the double functionalization reaction TEM analysis was carried out for **7** (Figure 6a). No substantial differences between the two different types of aggregates, **4b** and **7**, could be detected, although the images confirmed that the functionalization process greatly reduced the size of the bundles of pristine SWCNTs. Similarly to aggregates **4a,b**, quaternization of the imidazole rings of **6** by using Br^- as counter anion provides water soluble functionalizad SWCNTs. Whereas, SWCNTs substituted with the lipophilic anion PF_6^- are soluble in organic solvents such as DCM (Figure 6b).

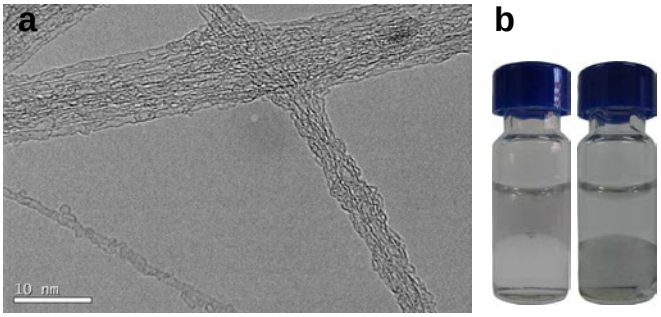

Figure 6. a) . TEM micrograph of **7** (scale bar 10 nm).b) Photographs of **7** with Br^- (left) or PF_6^- in H_2O (upper phase) and CH_2Cl_2 (lower phase) mixtures.

A final analysis about the nature and relative amount of the covalent chemical functionalities of **7** was completed using XPS (Figure S13). The survey spectra recorded for this material show the signals collected from C 1s (284.6 eV); O 1s (533.2 eV); N 1s (399.7 eV) and F 1s (689.7 eV). The relatively low amount of functional groups introduced by direct alkylation in the SWCNTs surface explains the lack of P signal. XPS also shown that, unfortunately, this methodology has produced undesirable side fluorinations reactions as could be observed for the great amount of F 1s present on the survey spectrum. The peak could be deconvoluted in two components, the intense peak at 689.4 eV corresponds to PF_6^- counter anion and a minor component at 691.0 eV, assigned to the direct attachment of the fluorine to the carbon atoms. This side reaction is also observable in the carbon signal through a C-F peak at 292.2 eV (insert in Figure S13).[30]

The high-resolution C 1s core level spectrum of **7** (insert in Figure S13) was satisfactorily fitted to five components as expected.[25] The most intense peak at 284.4 eV is due to sp^2 C–C bonds of graphitic carbon whereas the component at 284.9 eV is originated from sp^3 C–C bonds. The next three components at 285.6, 286.1 and 288.9 eV have been often assigned to C–O, C=O and COO groups.[31] In addition, **7** displays a weak component at around 291.4 eV corresponding to π–π* shake up transition of carbon atoms in graphene structures. Finally, as previously mentioned for **4b**, two weak C–N and C≡N components should be expected; however they are probably overshadowed by the strongest oxygenated bonds.

The N 1s spectrum exhibits a broad peak at 399.4 eV that could be fitted to two different contributions (insert in Figure S13). The cyano contribution from the TCAQ units is centred at 399.8 eV whereas the contribution centred at 401.5 eV could be assigned to the photoelectrons emitted from a quaternary N atom.[32] As for aggregates **4b**, the acceptor character of the TCAQ is evidenced in the present aggregate through an increasing of the cyano groups binding energy of ~ 1.1–1.8 eV compared with reference TCNQ or *p*-extended TCNQ reference systems.[17b,27]

Conclusions

In summary, we describe herein the synthesis and characterization of multifunctionalized SWCNTs bearing two different organic addends that may improve the SWCNTs properties: i) the imidazolium cation-based ionic liquid to infer different solubility on the material through counter anion exchange and, ii) the electron-acceptor TCAQ molecule. The influence of the organic function position has been studied using two different synthetic methodologies that consider several reactions to anchor the active molecules, namely a 1,3-dipolar cycloaddition reaction, amidation or esterification of carboxylic acid groups and, the use of diazonium salt (Tour reaction). We demonstrate that the second approach, which includes a direct sidewall functionalization using a diazonium salt methodology with the primary amine *N*-methyl imidazole provides a comparatively lower number of imidazolium units on the SWCNTs surface. Both facile and efficient strategies have allowed obtaining SWCNTs with tunable polarity between organic solvents and water. Furthermore, as XPS analysis seem to indicate, the strong electron-acceptor character of the TCAQ molecule may induce a *p*-type dope of the SWCNTs in solution. The multi-functionalized SWCNTs were unambiguously characterized by TEM, TGA, FTIR, Raman, XPS and UV-vis-NIR spectroscopy.

Experimental Section

Materials: HiPCO SWCNTs were purchase from Carbon Nanotechnologies Inc. (lot: P0343, purity >9 3 %, < 7 % remaining iron particles, length = 100 - 1000 nm, diameter = 0.8 - 1.2 nm). Organic solvents and reagents used in this work were purchase from Aldrich or Across organics and used as received, unless stated otherwise. Reactions involving water-sensible intermediates like SWCNTs functionalized with acid chloride were conducted under argon atmosphere, using standard Schlenk and vacuum-line techniques. Anhydrous organic solvents used in the functionalization of carbon nanotubes were previously purified by means of distillation under argon atmosphere with the appropriate drying agent (sodium/benzophenone for tetrahydrofuran). 2-formyl-11,11,12,12-tetracyano-9,10-anthra-*p*-quinodimethane and 2-hydroxymethyl-11,11,12,12-tetracyano-9,10-anthra-*p*-quinodimethane were synthesized following the previously reported methods.[33]

Instruments: Infrared spectra were carried out using pellets of dispersed samples of the corresponding compounds in dried KBr. The instrument used was a Bruker TENSOR FTIR. The spectral range was 4000-400 cm^{-1}. Thermogravimetric analyses were carried out under air and nitrogen in a TA-TGA-Q500 apparatus. The sample (~ 0,5 mg) was introduced inside a platinum crucible and equilibrated at 90 ºC followed by a 10 °C min^{-1} ramp between 90 and 1000 °C. XPS analyses were carried out using a SPECS GmbH (PHOIBOS 150 9MCD) spectrometer operating in the constant analyzer energy mode. A nonmonochromatic aluminium X-ray source (1486.61 eV) was used with a power of 200 W and voltage of 12 kV. Pass energies of 75 and 25 eV were used for acquiring both survey and high resolution spectra, respectively. Survey data were acquired from kinetic energies of 1487 - 400 eV with an energy step of 1 eV and 100 ms dwell time per point. The high resolution scans were taken around the emission lines of interest with 0.1 eV steps and 100 ms dwell time per point. SpecsLab Version 2.48 software was used for spectrometer control and data handling. The semi-quantitative analysis were performed from the C1s (284.3 eV) signal. The samples were introduced as pellets of 8 mm diameter. Raman spectra were recorded on Renishaw in Via Microscope at room temperature using two different exciting laser sources (785 and 532 cm^{-1}). TEM micrographs were obtained using a JEOL 2100 microscope operating at 200 kV. The SWCNTs samples were dispersed in organic solvents as DMF or NMP and sonicated for 5 minutes, the resulting suspension was dropped onto a holey carbon copper grid (200 mesh), and the solvent was allowed to evaporate.

Synthesis of SWCNTs–COOH (1): Pristine SWCNTs (400 mg) were dispersed onto HNO_3 6N (100 mL) using an ultrasound bath sonicator. The dispersion was then refluxed at 130 ºC during 24 hours and further filtered through a polycarbonate membrane and washed with distilled water until a stable pH value was reached (~6). IR (KBr): ν = 2900 (C-H stretching), 1730 (C=O, acid), 1592 (C-H vibration in plane) and 1200 (C–O stretching) cm^{-1}; TGA: weight loss and temperature desorption (decomposition): 10.92 %, 250 °C (carboxylic acid functionalities thermal decomposition); Raman: I_D/I_G = 0.23; XPS: % atomic: C (284.7 eV) = 82.39, O (532.3 eV) = 17.61.

Amidation of the SWCNTs surface (2): Oxidized SWCNTs **1** (400 mg) were refluxed in a solution of thionyl chloride (40 mL) for 24 hours at 70 °C under argon atmosphere; the solvent was then evaporated using argon as carrier gas. The chlorinated SWCNTs-COCl sample was reacted with 1-(3-aminopropyl)imidazole (40 mL) at 120 °C for 24 hours under argon atmosphere. The solid was separated by filtration through a 0.2 µm poly(tetrafluoroethylene) (PTFE) membrane and washed successively with THF followed by consecutive washings with 1 M aqueous HCl solution, saturated aqueous $NaHCO_3$ solution and water until the pH of the filtrate was 7.0. The resulting solid was finally washed with ethanol and dried overnight on the membrane filter. Wf **2** = 447 mg. IR (KBr): ν: = 2900 (C-H stretching), 1730 (C=O, acid), 1668 (C=O, amide), 1592 (C-H vibration in plane) and 1200 (C–O stretching) cm^{-1}; TGA: weight loss and temperature desorption (decomposition): 24.53 %, 385 °C (imidazole functionalities thermal decomposition); Raman: I_D/I_G = 0.24; XPS: % atomic: C (284.7 eV) = 81.22, O (532.3 eV) = 12.38, N (399.5eV) = 6.39.

1, 3-Dipolar cicloaddition functionalization of the SWCNTs surface (3a,b): SWCNTs **2** (25 mg) were suspended in dichloromethane and *N*-methylglycine (60 mg) and cyanobenzaldehyde (90 mg) were added, with a further solvent evaporation. The reaction was carried out under microwave irradiation in a closed quartz tube with control of pressure. Different ramp temperatures were used (Table 1) to avoid the high microwave absorption displayed in the absence of solvents. After cooling to room temperature, the solid was washed by filtration over a 0.2 µm poly(tetrafluoroethylene) (PTFE) membrane several times with DMF, CH_2Cl_2, and methanol (sonicated, centrifugated and filtered) until the filtrated solution remained colourless affording functionalized SWCNTs **3a**. Wf **3a** = 24.8 mg

Table 1. Irradiation steps used at the microwave reactor.

Step	Temperature (ºC)	Ramp time (min.)	Hold time (min.)
1	80	3	5
2	130	3	5
3	145	3	5
4	160	3	50

The preparation of nanoconjugates **3b** did not take place under microwave irradiation and a modified procedure was developed: 30 mg of **2** were suspended in 1,2-dichlorobenzene (*o*-DCB) and, *N*-methylglycine (302 mg) and 2-formyl-11,11,12,12-tetracyano-9,10-anthra-*p*-quinodimethane (60 mg) added. The reaction mixture was sonicated in a horn ultrasonicator processor for 48 hours. After cooling to room temperature, the suspension was filtered on a 0.2 µm poly(tetrafluoroethylene) (PTFE) membrane and the black solid was washed several times with DMF, CH_2Cl_2, and methanol (sonicated, centrifugated and filtered) until the filtrated solution remained colourless affording **3b**. Wf 3b = 35.8 mg.
IR (KBr): ν (**3a** and **3b**) =: 2900 (C-H stretching), 2226 (C≡N, nitrile), 1730 (C=O, acid), 1668 (C=O, amide), 1592 (C-H vibration in plane) and 1200 (C-O stretching); TGA: weight loss and temperature desorption (decomposition) cm^{-1}: 27.60 %, 350 °C (organic functionalities thermal decomposition) for **3a**, 24.53 %, 380 °C (organic functionalities thermal decomposition) for **3b**; Raman: I_D/I_G = 0.28 for **3a**, I_D/I_G = 0.27 for **3b**.
Alkylation reaction on SWCNTs surface (5): Activated SWCNTs **1** (25 mg), were dispersed in desionizated water (30 mL) using an ultrasonicator horn for fifteen minutes. The dispersion was then desoxigenated using argon for 10 minutes. 1-(3-aminopropyl)imidazole (25 µl) and isopenthyl nitrite (50 µl) were added to the mixture and then heated at 80 ºC under argon atmosphere overnight. The solid was filtered through a 0.2 µm PTFE membrane and washed with CH_2Cl_2 and methanol (sonicated, centrifugated and filtered) until the filtrated solution remained colourless. Wf **5** = 24.9 mg. IR (KBr): ν = 2900 (C-H stretching), 2226 (C≡N, nitrile), 1730 (C=O, acid), 1592 (C-H vibration in plane) and 1200 (C-O stretching) cm^{-1}; TGA: weight loss and temperature desorption (decomposition): 26.37 %, 400 °C (imidazole and carboxilic acid functionalities thermal decomposition); Raman: I_D/I_G = 0.15.
Esterification reaction on SWCNTs surface (6): The modified SWCNTs **5** (12 mg) were refluxed in a solution of thionyl chloride (10 mL) for 24 hours at 70 °C under argon; the solvent was then evaporated using argon as carrier gas. The chlorinated SWCNTs were without further purification re-dissolved in anhydrous THF (20 ml) and reacted with 2-hydroxymethyl-11,11,12,12-tetracyano-9,10-anthra-*p*-quinodimethane (12 mg) at 120 °C for 24 hours under argon atmosphere. The solid was separated by filtration through a 0.2 µm poly(tetrafluoroethylene) (PTFE) membrane and washed successively with THF followed by consecutive washings with 1 M aqueous HCl solution, saturated aqueous $NaHCO_3$ solution and water until the pH of the filtrate was 7.0. The resulting solid was finally washed with ethanol and dried overnight on the membrane filter to obtain **6**. Wf **6** = 17.4 mg. IR (KBr): ν = 2900 (C-H stretching), 2226 (C≡N, nitrile), 1740 (C=O, ester), 1592 (C-H vibration in plane), and 1200 (C-O stretching) cm^{-1}; TGA: weight loss and temperature desorption (decomposition): 20.73 %, °C (carboxylic acid functionalities thermal decomposition); Raman: I_D/I_G = 0.14.
Ionic functionalization of the SWCNTs surface (4a,b and **7):** 1-bromobutane (5 mL) was added to functionalized carbon nanotubes **3a** (25 mg), **3b** (35 mg) or **6** (10 mg) dispersed in *N*,*N*-dimethylformamide (DMF) (5 mL) and sonicated for 2 hours under nitrogen atmosphere in a bath sonicator. Afterwards the reaction was stirred at 80 °C for 24 hours under nitrogen atmosphere. The solid was separated by filtration through 0.2 µm PTFE membrane and thoroughly washed with THF several times to remove the excess of bromobutane. The anion exchange of Br^- by PF_6^- was obtained mixing the resulting solid (30 mg) with an aqueous solution of KPF_6 (300 mg in 50 mL of purified water). The mixture was stirred at room temperature for 24 hours. The solid was separated by filtration and washed with water to remove the water soluble species such as KBr. After several washings with water, the resulting solid **4a**, **4b**, or **7** was dried overnight in the membrane. Wf **4a** = 22.9 mg; Wf **4b** = 23.5 mg; Wf **7** = 12.7 mg. IR (KBr): ν = 2900 (C-H stretching), 2226 (C≡N, nitrile), 1730 (C=O, acid), 1668 (C=O, amide), 1592 (C-H vibration in plane), 1200 (C-O stretching) and 838 (P-F stretching) for **4a** and **4b** in cm^{-1}. ν = 2900 (C-H stretching), 2226 (C≡N, nitrile), 1740 (C=O, ester), 1592 (C-H vibration in plane), 1200 (C–O stretching) and 840 (P-F stretching) for **7** in cm^{-1}; TGA: weight loss and temperature desorption (decomposition): 31.93 %, 650 °C (ionic functionalities thermal decomposition) **4a**, 39.11 %, 573 ºC (ionic functionalities thermal decomposition) **4b**, 34.20 %, 650 °C (ionic functionalities thermal decomposition) 7; Raman: I_D/I_G = 0.26 for **4a**, I_D/I_G = 0.31 for **4b**, I_D/I_G = 0.16 for **7**. XPS: % atomic: C (284.7 eV) = 67.49, O (532.3 eV) = 20.68, N (399.5eV) = 5.18, F (689.1 eV) = 6.63 for **4a**; C (284.7 eV) = 67.41, O (532.3 eV) = 23.31, N (399.5eV) = 5.35, F (689.1 eV) = 3.92 for **4b**; C (284.7 eV) = 62,95, O (532.3 eV) = 23.70, N (399.5eV) = 1.39, F (689.1 eV) = 9.40 for 7.

Acknowledgements

Financial support from the European Research Council ERC-2012-ADG_20120216 (Chirallcarbon), MINECO of Spain (grant numbers CTQ2011-24652, PIB2010JP-00196, 2010C-07-25200, and Consolider-Ingenio CSD2007-00010), FUNMOLS (grant number FP7-212942-1), and CAM (grant number MADRISOLAR-2 S2009/PPQ-1533) is greatly appreciated.

[1] S. Iijima, *Nature* **1991**, *354*, 56–58.

[2] a) M. S. Dresselhaus, G. Dresselhaus, P. Avouris, *Carbon Nanotubes: Synthesis, Structure, Properties and Applications*, Springer, Berlin, **2001**; b) A. Jorio, G. Dresselhaus, M. S. Dresselhaus, *Carbon Nanotubes: Advanced Topics in the Synthesis, Structure, Properties and Applications*, Springer, Berlin, **2008**.

[3] a) M. T. Byrne, Y. K. Gun'ko, *Adv. Mater*. **2010**, *22*, 1672–1688; b) F. M. Toma, A. Sartorel, M. Iurlo, M. Carraro, P. Parisse, C. Maccato, S. Rapino, B. Rodriguez-Gonzalez, H. Amenitsch, T. Da Ros, L. Casalis, A. Goldoni, M. Marcaccio, G. Scorrano, G. Scoles, F. Paolucci, M. Prato, M. Bonchio, *Nat. Chem.* **2010**, *2*, 826–831; c) J. M. Lee, J. S. Park, S. H. Lee, H. Kim, S. Yoo, S. O. Kim, *Adv. Mater*. **2011**, *23*, 629–633; d) G. Magadur, J.-S. Lauret, G. Charron, F. Bouanis, E. Norman, V. Huc, C.-S. Cojocaru, S. Gomez-Coca, E. Ruiz, T. Mallah, *J. Am. Chem. Soc*. **2012**, *134*, 7896–7901; e) B. Esser, J. M. Schnorr, T. M. Swager, *Angew. Chem.* **2012**, *124*, 5851–5855; *Angew. Chem. Int. Ed.* **2012**, *51*, 5752–5756; f) E. S. Andreiadis, P.-A. Jacques, P. D. Tran, A. Leyris, M. Chavarot-Kerlidou, B. Jousselme, M. Matheron, J. Pécaut, S. Palacin, M. Fontecave, V. Artero, *Nature Chem.* **2013**, *5*, 48-53.

[4] a) M. Sharon, M. Sharon, *Carbon Nano Forms and Applications*, McGraw-Hill, New York, **2010**; b) D. M. Guldi, N. Martín, *Carbon nanotubes and related structures*, Wiley-VCH, Weinheim, **2010**; c) T. Akasaka, F. Wudl, S. Nagase, *Chemistry of Nanocarbons*, John Wiley&Sons, Chichester, **2010.**

[5] a) A. Hirsch, O. Vostrowsky, *Top. Curr. Chem.* **2005**, *245*, 193-237; b) G. Clavè, S. Campidelli, *Chem. Sci.*, **2011**, *2*, 1887–1896; c) F. Hof, S. Bosch, S. Eigler, F. Hauke, A. Hirsch, *J. Am. Chem. Soc.* **2013**, *135*, 18385–18395; d) K. Dirian, M. A. Herranz, G. Katsukis, J. Malig, L. Rodríguez-Pérez, C. Romero-Nieto, V. Strauss, N. Martín, D. M. Guldi, *Chem. Sci*., **2013**, *4*, 4335–4353.

[6] a) P. Wasserschied, T. Welton, *Ionic Liquids in Synthesis*, VCH–Wiley, Weinheim **2002**; b) R. Giernoth, *Angew. Chem.* **2010**, *122*, 2896–2901; *Angew. Chem. Int. Ed.* **2010**, 49 2834-2839.

[7] K. R. Seddon, *Ionic Liquids as Green Solvents*, ACS symposium Series 856, American Chemical Society, Washington, DC, **2003**.

[8] Y. Zhang, Y. Shen, J. Yuan, D. Han, Z. Wang, Q. Zhang, L. Niu, *Angew. Chem.* **2006**, *118*, 5999–6002*; Angew. Chem. Int. Ed*. **2006**, *45*, 5867-5870.

[9] M. J. Park, J. K. Lee, B. S. Lee, Y.-W. Lee, I. S. Choi, S-G. Lee, *Chem. Mater*. **2006**, *18*, 1546-1551.

[10] a) T. Fukushima, A. Kosaka, Y. Ishimura, T. Yamamoto, T. Takigawa, N. Ishii, T. Aida, *Science* **2003**, *300*, 2072–2074; b) T. Fukushima,; T. Aida, *Chem. Eur. J*. **2007**, *13*, 5048–5058.

[11] N. Hameed, J. S. Church, N. V. Salim, T. L. Hanley, A. Aminia, B. L. Fox, *RSC Adv*. **2013**, *3*, 20034–20039.

[12] a) F. G. Brunetti, M. A. Herrero, J. de M. Muñoz, A. Díaz-Ortiz, J. Alfonso, M. Meneghetti, M. Prato, E. Vázquez, *J. Am. Chem. Soc.* **2008**, *130*, 8094–8100; b) N. Rubio, M. A. Herrero, A. de la Hoz, M. Meneghetti, M. Prato, E. Vázquez, *Org. Biomol. Chem.* **2010**, *8*, 1936–1942.

[13] a) W. Wu, S. Wieckowski, G. Pastorin, M. Benincasa, C. Klumpp, J.-P. Briand, R. Gennaro, M. Prato, A. Bianco, *Angew. Chem.* **2005**, *117*, 6516–6520; *Angew. Chem. Int. Ed.* **2005**, *44*, 6358–6362; b) C. Fabbro, H. Ali-Boucetta, T. Da Ros, K. Kostarelos, A. Bianco, M. Prato, *Chem. Commun.* **2012**, *48*, 3911–3926.

[14] C. Ménard-Moyon1, C. Fabbro, M. Prato, A. Bianco, *Chem. Eur. J.* **2011**, *17*, 3222–3227.

[15] a) C. Backes, C. D. Schmidt, K. Rosenlehner, F. Hauke, J. N. Coleman, A. Hirsch, *Adv. Mater.* **2010**, *22*, 788–802; b) T. Umeyama, H. Imahori, *J. Phys. Chem. C*, **2013**, *117*, 3195–3209.

[16] C. Romero-Nieto, R. García, M. A. Herranz, L. Rodríguez-Pérez, M. Sánchez-Navarro, J. Rojo, N. Martín, D. M. Guldi, *Angew. Chem.* **2013**, *125*, 10406–10410; *Angew. Chem. Int. Ed.* **2013**, *52*, 10216–10220.

[17] a) J. Santos, E. M. Pérez, B. M. Illescas, N. Martín, *Chem. Asian J.* **2011**, *6*, 1848-1853; b) C. Urban, Y. Wang, J. Rodríguez-Fernández, R. García, M. A. Herranz, M. Alcamí, N. Martín, F. Martín, J. M. Gallego, R. Miranda, R. Otero, *Chem. Commun.* **2014**, *50*, 833–835.

[18] a) A. M. Kini, D. O. Cowan, F. Gerson, R. Mőckel, *J. Am. Chem. Soc.* **1985**, *107*, 556-562; b) A. Aumuller, S. Hunig, *Liebigs Ann. Chem*, **1984**, 618-621; c) N. Martin, R. Behnisch, M. Hanack, *J. Org. Chem.* **1989**, *54*, 2563 – 2568; d) J. Santos, B. M. Illescas, N. Martín, J. Adrio, J. C. Carretero, R. Viruela, E. Ortí, F. Spänig, D. M. Guldi, *Chem. Eur. J.*, **2011**, *17*, 2957-2964.

[19] a) Z. Yu, L.E. Brus, *J. Phys. Chem. A*, **2000**, *104*, 10995-10999; b) A. Kuznetsova, I. Popova, J. T. Yates, M. J. Bronikowski, C. B. Huffman, J. Liu, R. E. Smalley, H. H. Hwu, J. G. Chen, *J. Am. Chem. Soc.* **2001**, *123*, 10699-10704.

[20] S. Giordani, J.-F. Colomer, F. Cattaruzza, J. Alfonsi, M. Meneghetti, M. Prato, D. Bonifazi, *Carbon*, **2009**, *47*, 578-588.

[21] V. Georgakilas, K. Kordatos, M. Prato, D. M. Guldi, M. Holzinger, A. Hirsch, *J. Am. Chem. Soc.*, **2002**, *124*, 760-761.

[22] M. J. Park, J. K. Lee, B. S. Lee, Y.-W. Lee, I. S. Choi, S. G. Lee, *Chem. Mater.* **2006**, *18*, 1546-1551.

[23] B. Gebhardt, Z. Syrgiannis, C. Backes, R. Graupner, F. Hauke, A. Hirsch, *J. Am. Chem. Soc.* **2011**, *133*, 7985-7995.

[24] M. S. Strano, C. A. Dyke, M. L. Usrey, P. W. Barone, M. J. Allen, H. Shan, C. Kittrell, R. H. Hauge, J. M. Tour, R. E. Smalley, *Science* **2003**, *301*, 1519-1522.

[25] T .I. T. Okpalugo, P. Papakonstantinou, H. Murphy, J. McLaughlin, N. M. D. Brown, *Carbon*, **2005**, *43*, 153-151.

[26] M.T. Martínez, M.A. Callejas, A.M. Benito, M. Cochet, T. Seeger, A. Ansón, J. Schreiber, C. Gordon, C. Marhic, O. Chauvet, J. L.G. Fierro, W.K. Maser, *Carbon* **2003**, *41*, 2247–2256.

[27] P. Fesser, C. Iacovita, C. Wäckerlin, S. Vijayaraghavan, N. Ballav, K. Howes, J.-P. Gisselbrecht, M. Crobu, C. Boudon, M. Stöhr, T. A. Jung, F. Diederich, *Chem. Eur. J.* **2011**, *17*, 5246–5250.

[28] B. Yu, F. Zhou, G. Liu, Y. Liang, W. T. S. Huck, W. Liu, *Chem. Commun.* **2006**, 2356–2358.

[29] B. K. Price, J. M. Tour, *J. Am. Chem. Soc.* **2006**, *128*, 12899-12904.

[30] Y. S. Lee, T. H. Cho, B. K Lee, J. S. Rho, K. H. An, Y. H. Lee, *J. Fluorine Chem.* **2003**, *120*, 99–104.

[31] a) H. P. Boehm, *Carbon*, **2002**, *40*, 145-149; b) E. Del Canto, K. Flavin, D. Movia, C. Navio, C. Bittencourt, S. Giordani, *Chem. Mater*., **2011**, *23*, 67-74.

[32] D. Benne, E. Maccallini, P. Rudolf, C. Sooambar, M. Prato, *Carbon* **2006**, *44*, 2896–2903.

[33] a) B. M. Illescas, N. Martín, C. Seoane, *Tetrahedron Lett.* **1997**, *11*, 2015–2018; b) b) M. A. Herranz, B. Illescas, N. Martín, C. Luo, D. M. Guldi, *J. Org. Chem.* **2000**, *65*, 5728-5738.

Received: ((will be filled in by the editorial staff))

Revised: ((will be filled in by the editorial staff))

Published online: ((will be filled in by the editorial staff))

Dual function SWCNTs

L. Rodríguez-Pérez, R. García, M. A. Herranz, Nazario Martin
……..…

Modified SWCNTs with Amphoteric Redox and Solubilizing Properties

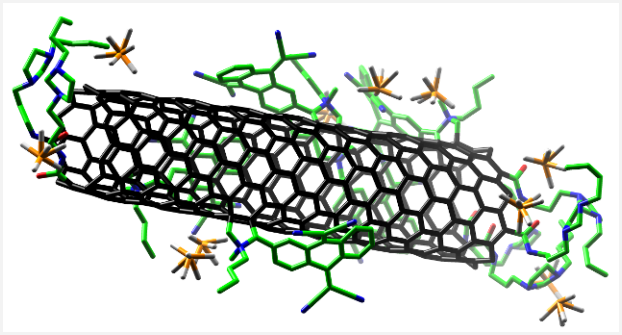

Incorporating two different functional groups as a TCAQ and an imidazolium based ionic liquid on SWCNTs gives birth to a potential electroactive material with tuneable hydrophilic/hydrophobic polarity by simply ion exchange. The functional groups position has been interchanged and further studied.

Supporting Information

Modified SWCNTs with Amphoteric Redox and Solubilizing Properties

Laura Rodríguez-Pérez,[a] Raúl García,[a] Mª Ángeles Herranz*[a] and Nazario Martín*[a, b]

[a] Departamento de Química Orgánica, Facultad de Química, Universidad Complutense de Madrid, 28040 Madrid (Spain). E-mail: maherran@quim.ucm.es, nazmar@quim.ucm.es

[b] IMDEA-Nanociencia, Facultad de Ciencias, Universidad Autónoma, Cantoblanco, 28049 Madrid, Spain.

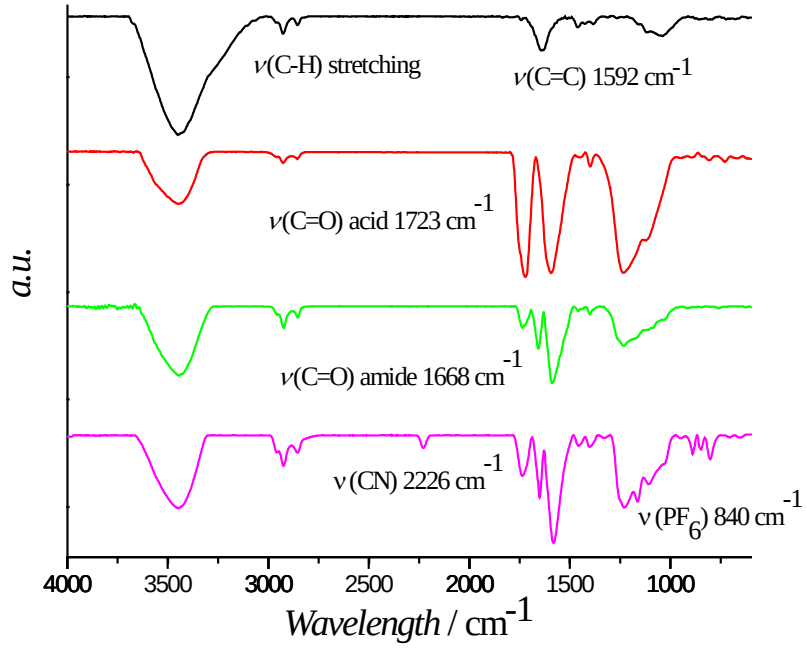

Figure S1. FTIR spectra of **4a** (magenta) compared to **2** (green), **1** (red) and pristine SWCNTs.

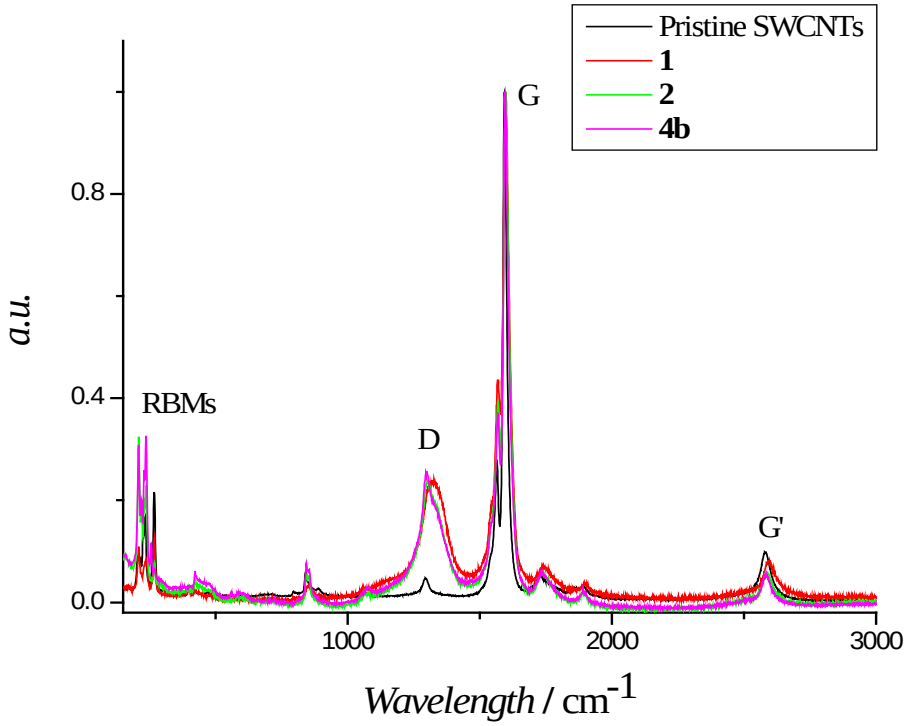

Figure S2. Raman spectra of pristine SWCNTs (black), oxidized SWCNTs (**1**) (red), **2** (green), and **4a** (magenta).

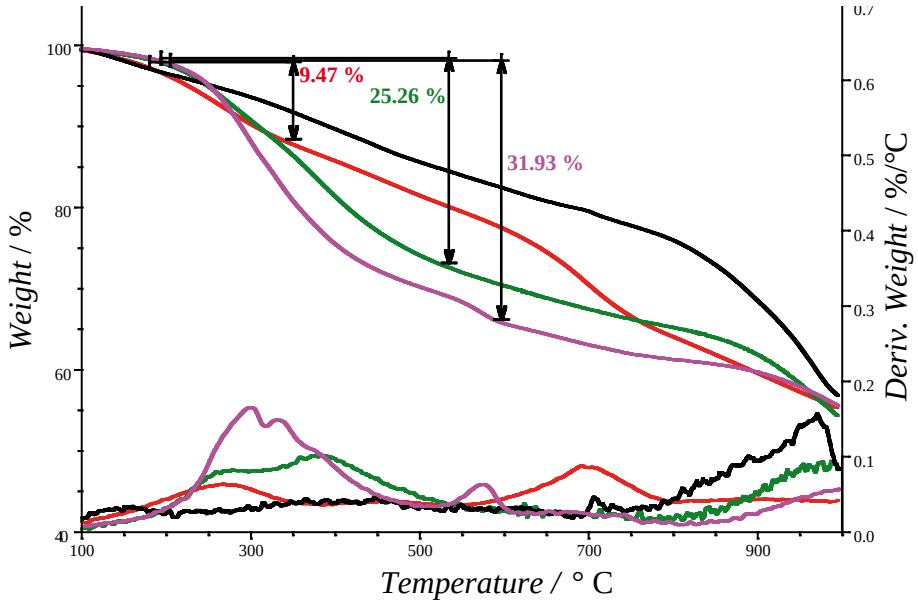

Figure S3. TGA analysis under inert atmosphere (nitrogen) of pristine SWCNTs (black), oxidized SWCNTs (**1**) (red), **2** (green) and **4a** (magenta).

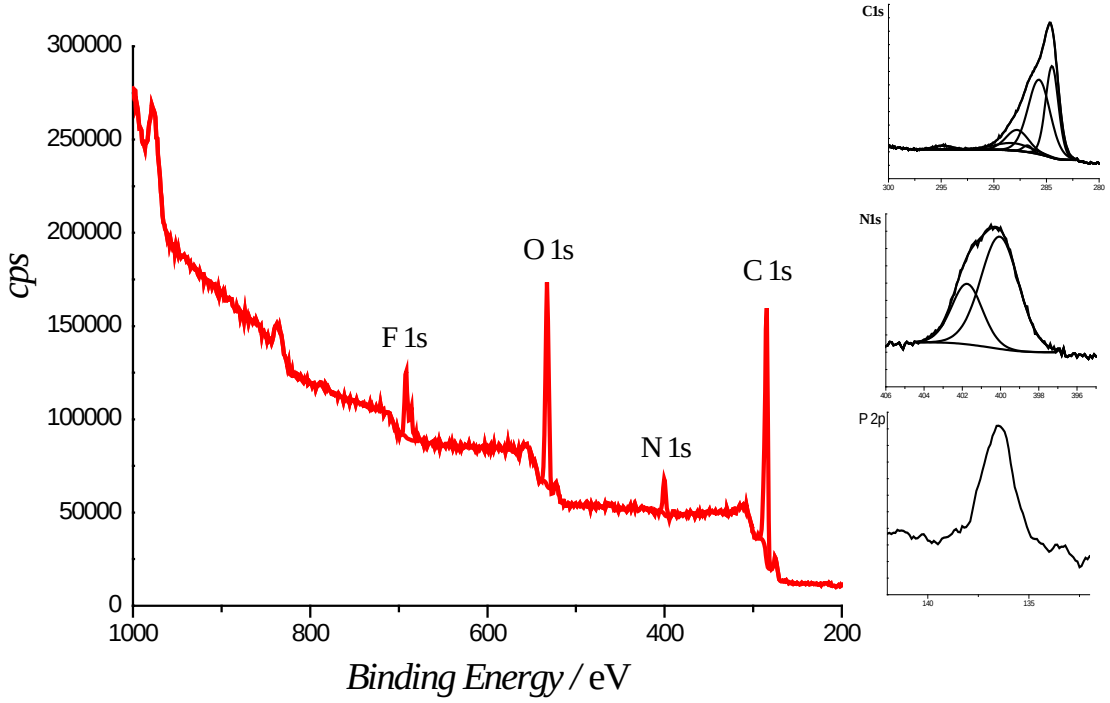

Figure S4. XPS analysis for **4a**, with the carbon, nitrogen and phosphorous components deconvolutions (inset right).

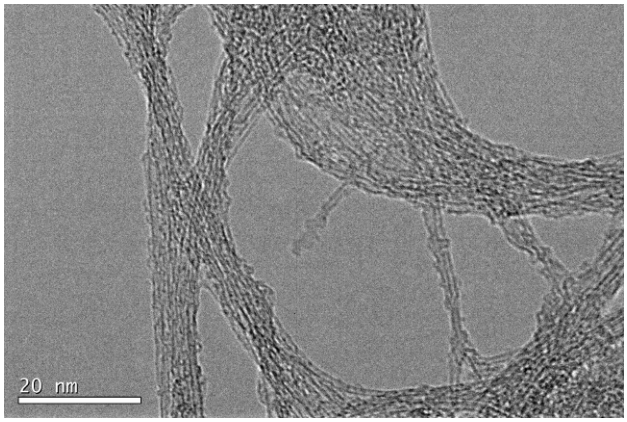

Figure S5. Representative TEM micrograph of **4a** (scale bar 20 nm).

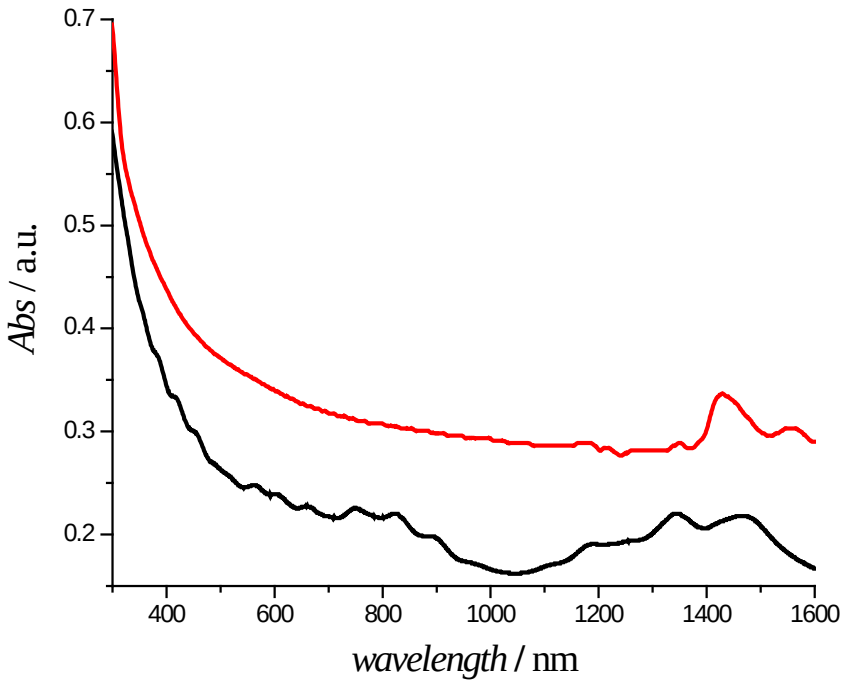

Figure S6. UV-vis spectra of **4b** compared to pristine SWCNTs where it can be observed the loss of the van Hove singularities.

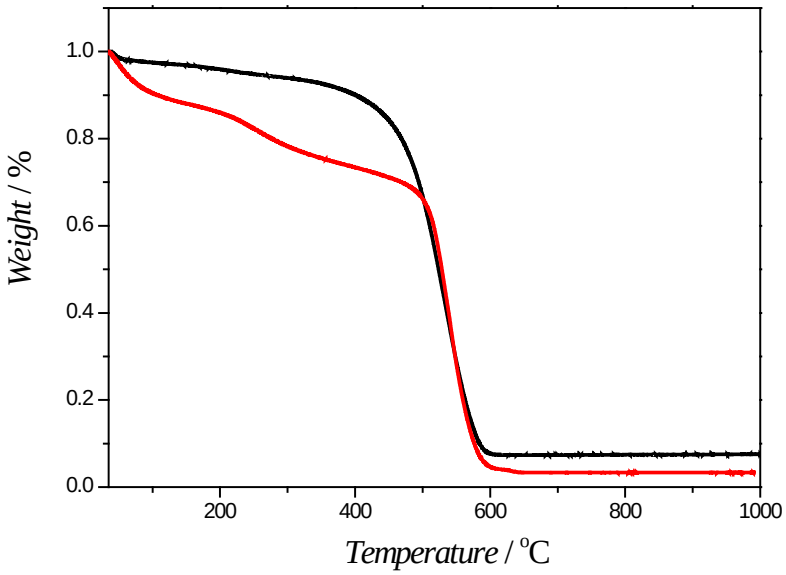

Figure S7. TGA analysis under air of pristine SWCNTs (black) and oxidized SWCNTs (**1**) (red).

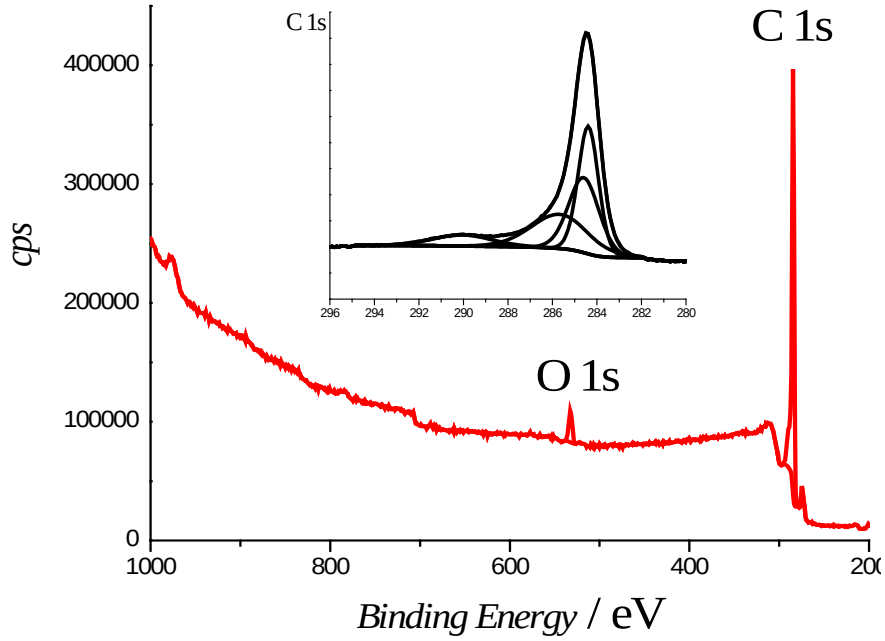

Figure S8. XPS analysis of pristine SWCNTs with the carbon atom component deconvolution.

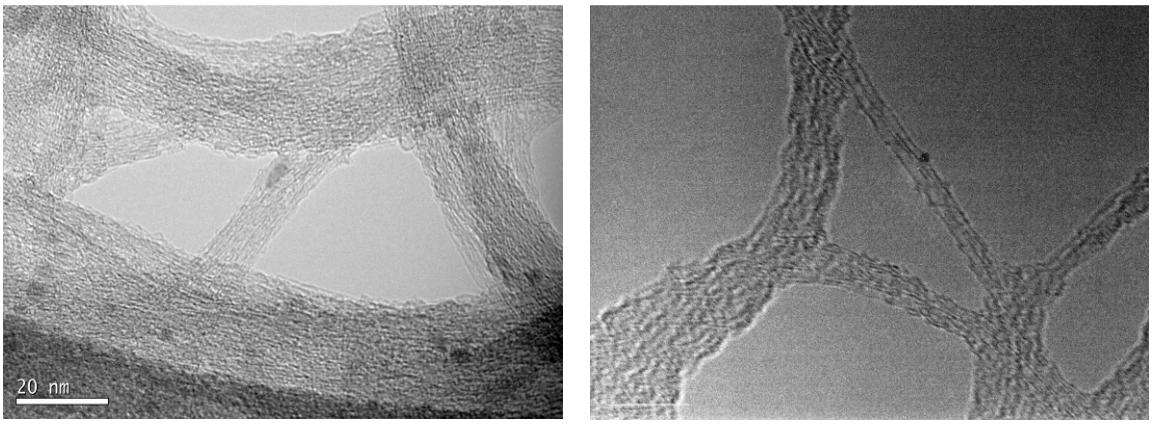

Figure S9. TEM micrograph of pristine SWCNTs (left) (scale bar 20 nm) and **4b** (right) (scale bar 10 nm)

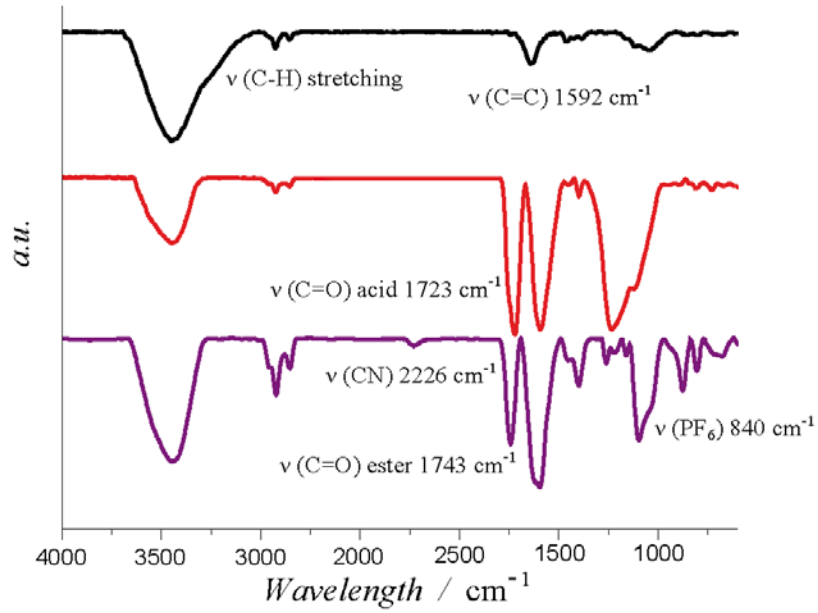

Figure S10. FTIR spectra of **7** (purple) compared to **1** (red) and pristine SWCNTs.

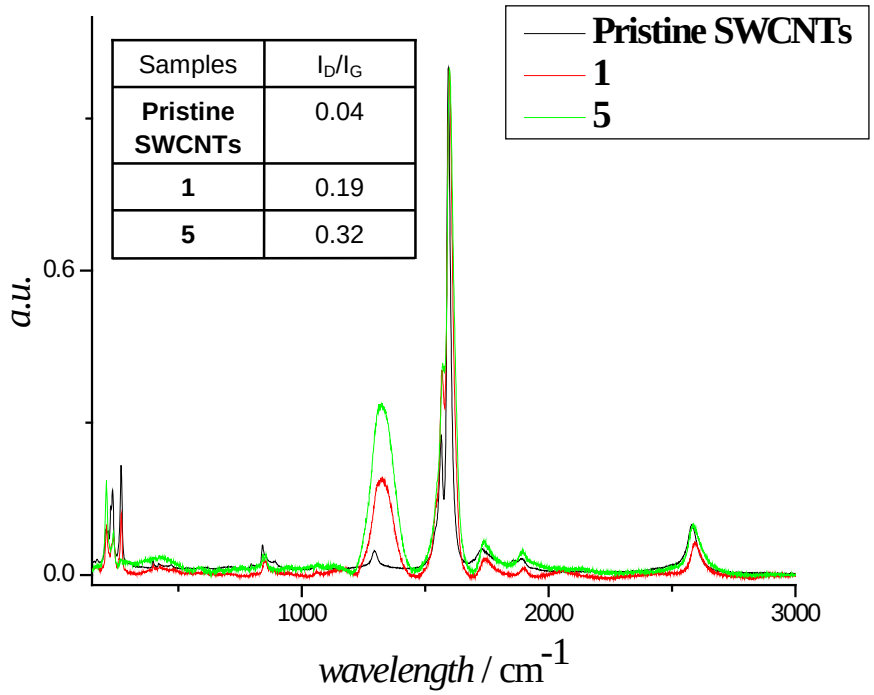

Figure S11. Raman spectra recorded at 785 nm of pristine SWCNTs (black), **1** (red) and **5** (green). The inset shows the I_D/I_G ratio.

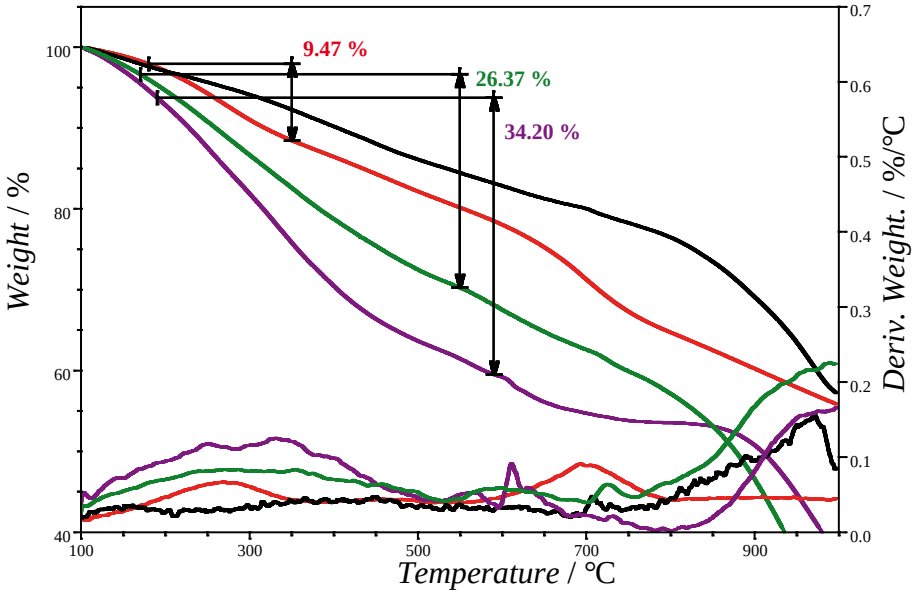

Figure S12. TGA analysis under inert conditions (nitrogen) of pristine SWCNTs (black), oxidized SWCNTs (**1**) (red), **5** (green) and **7** (purple).

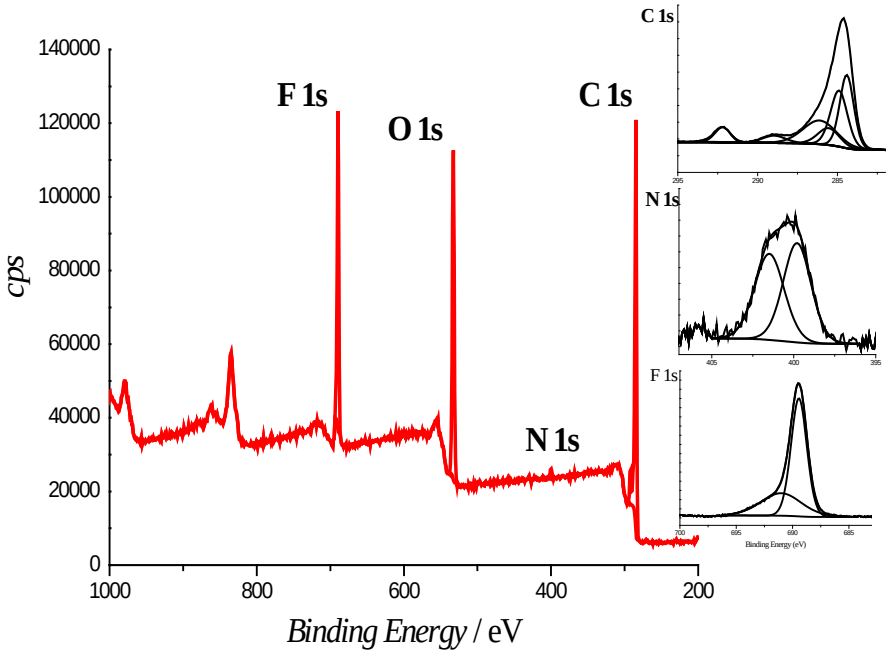

Figure S13. XPS analysis for **7**, with the carbon, nitrogen and fluor components deconvolutions (inset right).